Final Report for Award NASA NAG5-11880

Robert W. Schunk, Principal Investigator
Utah State University

Title: The Flow of Plasma in the Solar-Terrestrial Environment

Participant Individuals:

Jan J. Sojka, Co-Principal Investigator
Abdallah R. Barakat, Co-Investigator
Howard G. Demars, Co-Investigator
Lie Zhu, Co-Investigator

Goal

The overall goal of our NASA theory research is to *trace the flow of mass, momentum, and energy* through the magnetosphere-ionosphere-atmosphere system taking into account the *coupling, time delays,* and *feedback mechanisms* that are characteristic of the system. Our approach is to model the magnetosphere-ionosphere-atmosphere (M-I-A) system in a *self-consistent quantitative* manner using *unique global models* that allow us to study the coupling between the different regions *on a range of spatial and temporal scales.* The uniqueness of our global models stems from their high spatial and temporal resolutions, the physical processes included, and the numerical techniques employed. Currently, we have time-dependent global models of the *ionosphere, thermosphere, polar wind, plasmasphere,* and *electrodynamics.*

It is now becoming clear that a significant fraction of the flow of mass, momentum, and energy in the M-I-A system occurs on relatively small spatial scales. Therefore, an important aspect of our NASA Theory program concerns the effect that *mesoscale* (100-1000 km) density structures have on the macroscopic flows in the ionosphere, thermosphere, and polar wind. The structures can be created either by structured magnetospheric inputs (i.e., structured electric field, precipitation, or Birkeland current patterns) or by time variations of these inputs due to geomagnetic storms and substorms. Some of the mesoscale structures of interest include sun-aligned polar cap arcs, propagating plasma patches, traveling convection vortices, subauroral ion drift (SAID) channels, gravity waves, and the polar hole.

In the paragraphs that follow, we briefly highlight some of the studies we have recently conducted. A list of NASA publications is also attached.

Ionosphere-Polar Wind Coupling → Classical Outflow

The *classical* polar wind is an ambipolar outflow of thermal plasma from the terrestrial ionosphere at high latitudes. The outflow, which consists of H^+, He^+, and O^+, begins at about 800 km. As the ions flow up and out of the topside ionosphere along diverging geomagnetic field lines, they are accelerated and eventually become supersonic (above 1300 km). In addition, the upflowing ions convect horizontally across the polar region due to magnetospheric electric fields, moving in and out of sunlight, the auroral oval, and the polar cap. When integrated over

the polar regions, the polar wind corresponds to an important ionospheric loss process and an important source of magnetospheric plasma. The polar wind also interacts in a complex way with the hot magnetospheric plasma. Because of its importance, we have studied numerous polar wind features over the years, including its anisotropic thermal structure, its multi-ion character, its evolution through the collision-dominated to collisionless transition region, its interaction with hot magnetospheric electrons, its interaction with electrostatic waves, its ability to trap heavy ions, its stability, the conditions under which shocks can form and the effect of centrifugal acceleration.

During the last three years, our three-dimensional, time-dependent, fluid model was used to investigate the velocity structure of the global ionosphere-polar wind system. Simulations for solar maximum and minimum at both winter and summer were performed to evaluate the ionosphere-polar wind ion velocity morphology. Each simulation began under quiet geomagnetic conditions with cross-polar cap potentials of 33 kV and maximum auroral electron precipitation fluxes of 0.8 erg cm^{-2} s^{-1} which then increased to storm levels of 100 kV and 8 erg cm^{-2} s^{-1}. Results indicate that during all four simulations at 0600 UT, when the maximum storm conditions were reached, H^+ and O^+ ions were counter-streaming over much of the polar cap. H^+ ions were up-flowing with speeds of up to 12-20 km/s, while O^+ was down-flowing with speeds of 3-6 km/s (see Figure 1). The H^+-O^+ counterstreaming has important implications for the stability of the polar wind.

Ionosphere-Plasmasphere Coupling → Sub-Auroral Polarization Stream

Strong polarization electric fields develop across the sub-auroral ionosphere during active geomagnetic conditions and these electric fields drive Sub-Auroral Polarization Streams (SAPS). It has been shown by *Foster et al.* (*Geophys. Res. Lett*, 29, 2002) that storm enhanced densities (SED) and plumes of greatly elevated TEC are associated with the erosion of the outer plasmasphere by strong sub-auroral polarization electric fields. The SED/TEC plumes that are observed at low altitudes map closely onto the magnetospheric determination of the boundaries of the plasmapause and plasmaspheric tail (*Foster et al.*, 2002).

We used the USU Time Dependent Ionospheric Model (TDIM) in high-resolution mode, 0.2 degrees in latitude and 5 degrees in longitude, to study the impact of the Sub-Auroral Polarization Stream (SAPS). The SAPS convection electric field was obtained from observations made by the Millstone Hill incoherent scatter radar (J. Foster and co-workers, private communication, 2002). Figure 2 contrasts high-resolution regional magnetic latitude and magnetic local time distributions of N_mF_2 for no SAPS (top panel) and SAPS included (lower panel). The additional new density structures and associated steep horizontal gradients are a significant Space Weather feature that has impact on systems like the WAAS network. Furthermore, these plasma structures and their associated plasmapause flux tube structures are integrally related to magnetospheric detached plasma patches. These are plasma phenomena that are being observed by the NASA IMAGE satellite.

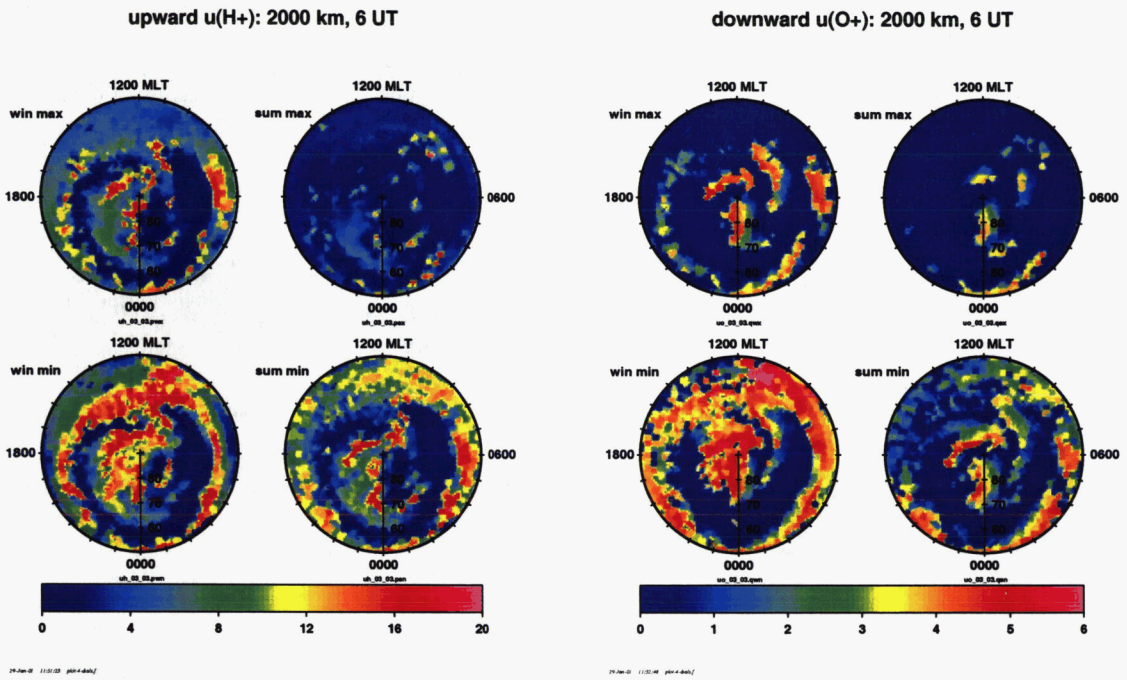

Figure 1. Shapshots of upward-flowing H^+ drift velocity distributions (left four panels) and downward flowing O^+ drift velocity distributions (right four panels). Each set of four panels corresponds to solar maximum (top row) and solar minimum (bottom row) for winter (left) and summer (right). Both velocity color keys are in km/s. (From Paper 10)

Ionosphere-Thermosphere Coupling → Plasma Bubbles

Mesoscale (100-1000 km) plasma structures are prevalent in the Earth's ionosphere. They occur in the form of propagating plasma patches, enhanced ionization channels associated with sun-aligned arcs, auroral and boundary blobs, and equatorial plasma bubbles. Because such structures can have an appreciable effect on the thermosphere, we have been conducting systematic modeling studies in order to determine their quantitative effect. Our studies are based on a *time-dependent, high-resolution* model of the *global ionosphere* that we developed several years ago. In one of our studies, we focused on the effects that equatorial plasma bubbles have on the thermosphere (Paper 16).

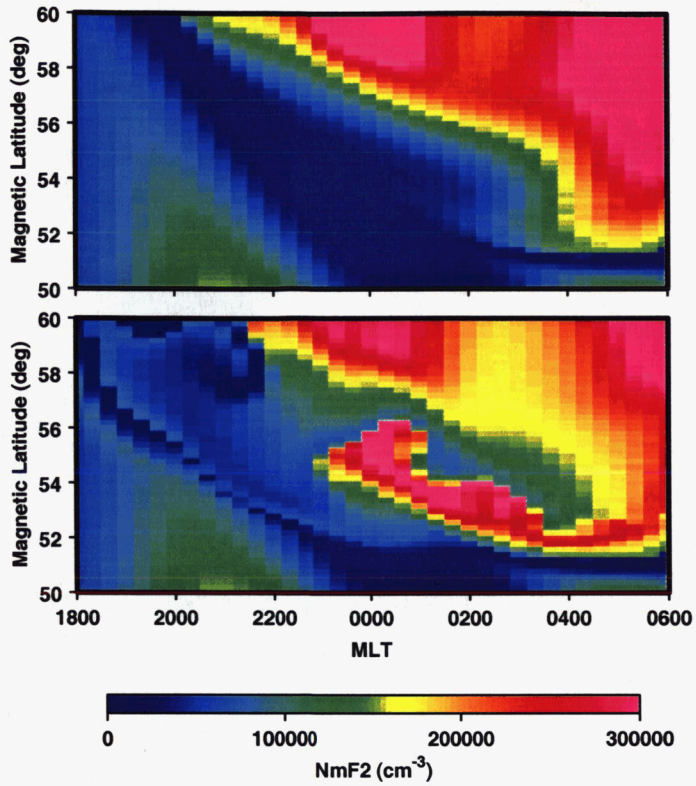

Figure 2. F-region N_mF_2 distributions for Volland convection (top panel) and for Volland plus SAPS convection (lower panel). (From Paper 8)

Equatorial plasma bubbles develop at dusk as a result of the Rayleigh-Taylor instability. After the R-T instability is triggered, bubbles form on the bottomside of the F-layer and then drift upward through the F-region and topside ionosphere. The bubbles take the form of vertically elongated wedges of depleted plasma, and the individual flux tubes in a vertical wedge are typically depleted along their entire north-south extents. The east-west extent of a disturbed region can be several thousand kilometers, with the horizontal distance between separate depleted regions being tens to hundreds of kilometers. When bubbles form, their upward drift typically varies from 100 to 500 m/s, but fast bubbles, with speeds in the range of from 500 m/s to 5 km/s, are not uncommon. The plasma depletion in the bubbles can be up to a factor of 1000 lower than that in the surrounding ionosphere. After formation, the vertical wedges of depleted plasma corotate with the Earth.

Using the USU Thermospheric General Circulation Model (TGCM) the meso-scale structuring associated with equatorial plasma bubbles was simulated. Bubbles were introduced at an hourly separation beginning at 2000 LT and allowed to develop over an hour, reaching apex heights of 1500 km. Each bubble had a one-hour local time depletion extent. Figure 3 shows both the relative thermospheric density impact (top

panel) as well as the temperature impact (bottom panel) of a series of bubbles in a geographic latitude and longitude format at an altitude of 300 km. This shows that these perturbations have a global extent spanning the equator from 30° N to 30° S, as well as persisting for over 6 hours in local time. The magnitude of the thermospheric density perturbations reaches 6% and are both enhancements and depletions, while the temperature deviations reach 35 K.

Ionosphere-Magnetosphere Coupling → Auroral Precipitation

It is well-known that auroral precipitation has an important effect on the high-latitude ionosphere. The energetic electrons are not only the source of optical missions, but also a source of heat for both the ionosphere and atmosphere. In addition, the precipitating electrons are a source of ionization owing to electron impact with the neutrals. The impact ionization builds up very rapidly and, as a consequence, both E and F region plasma density enhancements are seen in the auroral oval in association with the precipitation. Subsequently, the plasma created in the oval convects to other high-latitude regions. However, it is not known to what extent the aurorally-produced plasma contributes to the *background* plasma in the high-latitude ionosphere.

Recently, we used our global ionospheric model in an effort to determine the relative contributions of solar and auroral ionization to the overall background plasma in the polar region. The solar EUV production is readily modeled and is predictable, but in contrast, the aurorally-produced ionization is highly variable within the auroral oval. Nevertheless, we adopted empirical convection and precipitation models and conducted ionospheric simulations without auroral ionization and without solar production, and sample results are shown in Figure 4. The main conclusion of our study is that the auroral ionization provides an appreciable *baseline level* of polar cap F region plasma, upon which is superimposed the seasonally dependent tongue-of-ionization that extends into the polar cap from the dayside ionosphere.

Ionosphere-Magnetosphere Coupling → Substorms

Substorms correspond to an explosive release of energy in the auroral region near midnight magnetic local time. In a substorm, there are growth, expansion, and recovery phases, with the expansion phase typically lasting 30 minutes and the entire substorm about 2-3 hours. When viewed via the optical emission, the substorm first appears as a localized region of bright emission on the poleward edge of the auroral oval near local magnetic midnight. The so-called bulge is part of the westward traveling surge that occurs during the expansion phase of a substorm. Associated with substorms are locally enhanced electric fields, particle precipitation, and both field-aligned and electrojet currents. Eventually, the substorm-associated disturbances encompass the entire high-latitude region.

In studies of magnetosphere-ionosphere coupling and substorms, it has been conventionally assumed that the field-aligned currents are solely closed by the Pedersen currents in the ionosphere and that the Hall currents are divergence-free. By using the USU M-I electrodynamic model in which the electrodynamics is fully self-consistent via an Alfven wave approach, it was found that such an assumption, widely used by the space research community, can become invalid when the M-I system is disturbed, *especially during substorm periods.* In

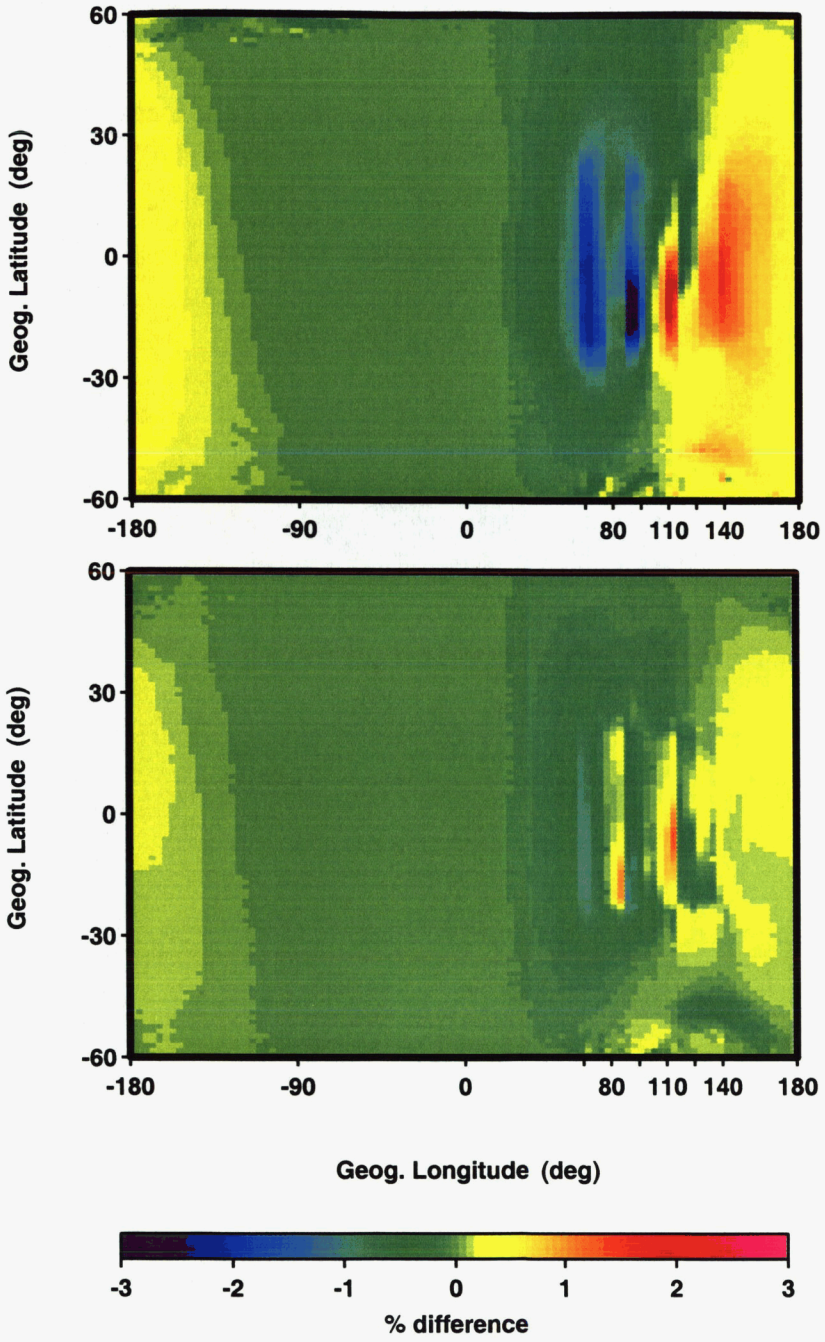

Figure 3. Thermospheric density perturbations at 300 km (top panel) and temperature perturbations (lower panel) associated with a series of four F-region equatorial plasma bubbles. (From Paper 16)

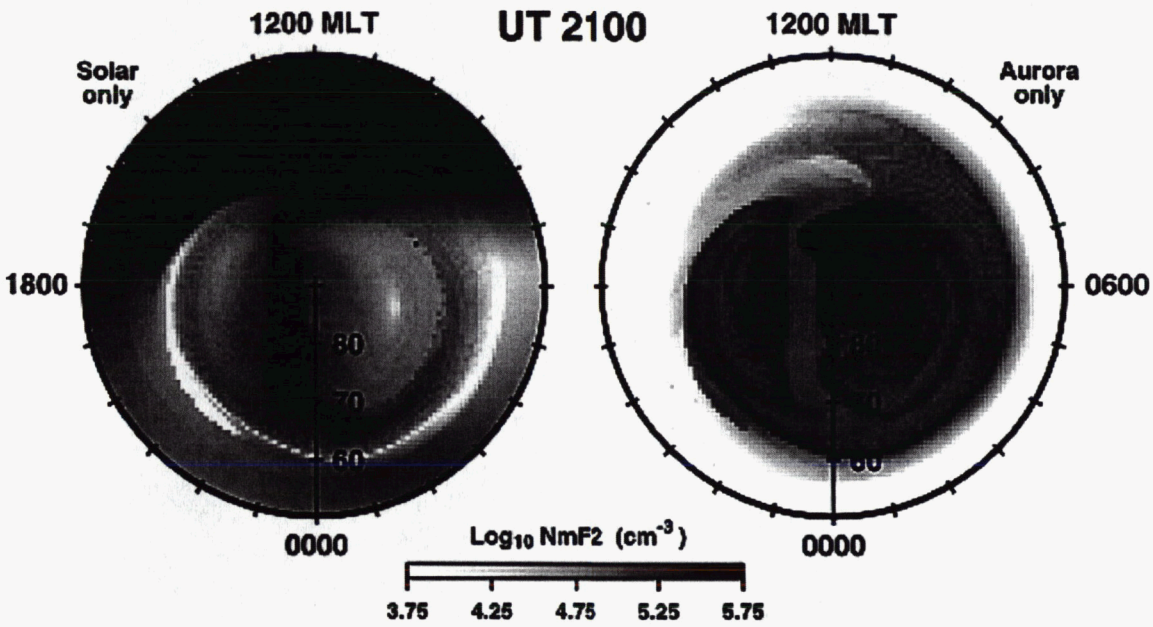

Figure 4. Two dial plot snapshots of simulated N_mF_2 over the Northern Hemisphere polar cap at 2100 UT in winter; the model was run (left) with no auroral input and (right) with no solar EUV input. The electron density is gray scaled as a log_{10} value over 2 orders of magnitude. A magnetic latitude and magnetic local time coordinate system is used. (From Paper 9)

the substorm onset regions, not only can the field-aligned currents be closed by the Hall currents, but the closure of these Hall currents can also lead to the development of small-scale electrodynamic structures (Figure 5). These small-scale electrodynamic structures, as well as the associated plasma structures, are essential for space weather studies.

Ionosphere-Polar Wind Coupling → Propagating Polar Wind Jets

Polar cap patches are regions of enhanced ionization that appear when the interplanetary magnetic field turns southward. They are created in the dayside cusp or equatorward of the cusp in the sunlit hemisphere. Once formed, they convect in an antisunward direction across the polar cap at the prevailing convection speed. The size of a plasma patch varies from about 200 to 1000 km, and its density relative to the background plasma density varies from a few percent to up to a factor of 100. A time-dependent, 3-dimensional model of the coupled ionosphere-polar wind system was used to study the effect that a "representative" plasma patch has on the polar wind. The model indicates that the enhanced O^+ densities in the propagating plasma patch leads to enhanced H^+ densities. As the plasma patch convects across the polar cap, H^+ flows up and out of the topside ionosphere with a supersonic velocity. Therefore, a plasma patch looks like a horizontally propagating, vertically directed, polar wind jet.

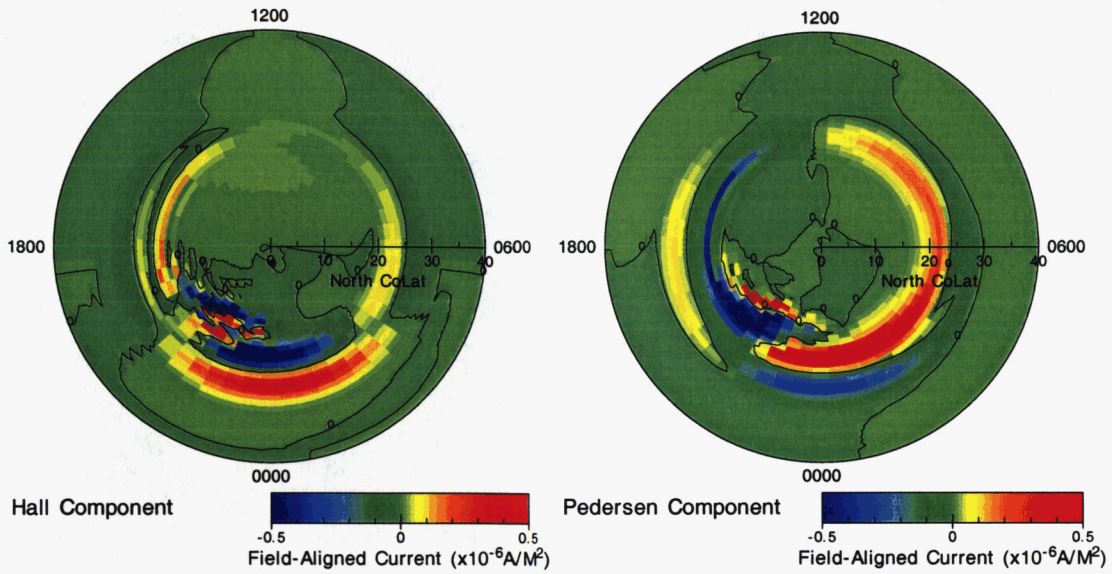

Figure 5. Distributions of the Pedersen and Hall components of the field-aligned currents during the expansion phase of substorms. In the substorm onset regions, the Hall components make a significant contribution and display small-scale structures.

The characteristics of propagating polar wind jets were studied with our 3-dimensional, time-dependent model of the ionosphere-polar wind system. In our study, a propagating plasma patch was 'imposed' on the background ionosphere at a certain UT and then its characteristics were modeled as it convected across the polar region with the background ionosphere. The patch was imposed at 0400 UT in the northern polar region on the dayside near local noon. A nearly circular patch was selected with a diameter of 1000 km. At the center of the patch the plasma density was a factor of 10 above the background plasma density, but this factor decreased in a Gaussian manner to 1 at the patch edge. Note that these patch characteristics are consistent with measurements. After the plasma patch was imposed, it convected across the polar cap with the background plasma in an antisunward direction at the prevailing convecting velocity. Figure 6 shows snapshots of the H^+ density distribution at 1000 km, and at 4, 5, 6, and 7 UT. The propagating plasma patch is seen as the 'red spot.' At 4 UT, it is nearly circular and located on the dayside at 1200 MLT, which is where it was imposed. As the plasma patch and background ionosphere convect, the plasma patch becomes distorted, because the convection streamlines that pass through the patch can have different convection speeds and directions associated with them. At 5 UT, the plasma patch is no longer circular, and at 6 UT it is located on the nightside between 80-90° magnetic latitude and midnight MLT. At 7 UT, the plasma patch is barely detectable and is located between 65-70° magnetic latitude at about 2200 MLT.

The altitude variation of the plasma patch (e.g., propagating polar wind jet) at 6 UT is shown in Figure 7. This figure is a color-coded contour plot of the H^+ density versus altitude and magnetic latitude from noon to midnight through the propagating polar wind jet. The enhanced H^+ densities between 76° and 90° magnetic latitude on the nightside correspond to the propagating polar wind jet. Note that the elevated H^+ densities extend all the way to the upper boundary. Without the propagating plasma patch, the polar wind jet would not exist and the H^+ density structure between 76°-90° would be similar to that in the low density region between 60°-76° on the nightside.

Polar cap patches, and hence propagating polar wind jets, are common at high latitudes when the IMF is southward, and frequently, multiple structures occur simultaneously. This implies that the mass loading of the magnetosophere due to ion outflow is even more irregular than perhaps has been anticipated. The nonuniform ion outflows in the polar cap and auroral oval should have an important effect on the evolution of geomagnetic storms and substorms in the magnetosphere. Our simulations provide further support to the growing impression that most of the mass, momentum, and energy coupling between the ionosphere and magnetosphere occurs on relatively small spatial scales.

Ionosphere-Exosphere Coupling → Neutral Polar Wind

The polar wind is an ambipolar outflow of ions from the terrestrial ionosphere at high latitudes. The polar wind, which consists of both thermal and energetic ions (H^+, O^+, He^+), begins at about 800 km. As the ions flow up and out of the topside ionosphere along diverging geomagnetic field lines, they are accelerated and eventually become supersonic. In addition, the upflowing ions convect horizontally across the polar region due to magnetospheric electric fields, moving in and out of sunlight, the auroral oval, and the polar cap. As the O^+ and H^+ ions flow upwards, they can undergo charge exchange reactions with the background neutral atmosphere (H and O), thereby creating energetic neutral particles (Figure 8). The initial velocity of the neutral particles is equal to the velocity of the H^+ and O^+ parent ions just before the charge exchange process. At high altitudes, neutral streams of H and O are created that predominately flow in the vertical direction (the neutral polar wind), while at low altitudes the neutral particles tend to move in all directions owing to horizontal plasma convection. In order to study this phenomenon, we developed a new polar wind model that self-consistently takes account of the neutrals H and O as well as the ions (H^+ and O^+). The results from our initial simulations (Paper 22) indicate that large escape fluxes of about 10^9 cm^{-2} s^{-1} can be expected for the neutral H stream for a range of seasonal and solar cycle conditions. However, the O stream particles tend to flow in the downward direction, because we did not include O^+ energization processes and, hence, the resulting O produced by charge exchange did not have sufficient energy to escape.

Ionosphere-Thermosphere Coupling → Theta Aurora

Mesoscale (100-1000 km) plasma structures are prevalent in the Earth's ionosphere. They occur in the form of propagating plasma patches, enhanced ionization channels associated with sun-aligned arcs, auroral and boundary blobs, and equatorial plasma bubbles. Because such structures can have an appreciable effect on the thermosphere, we have been conducting

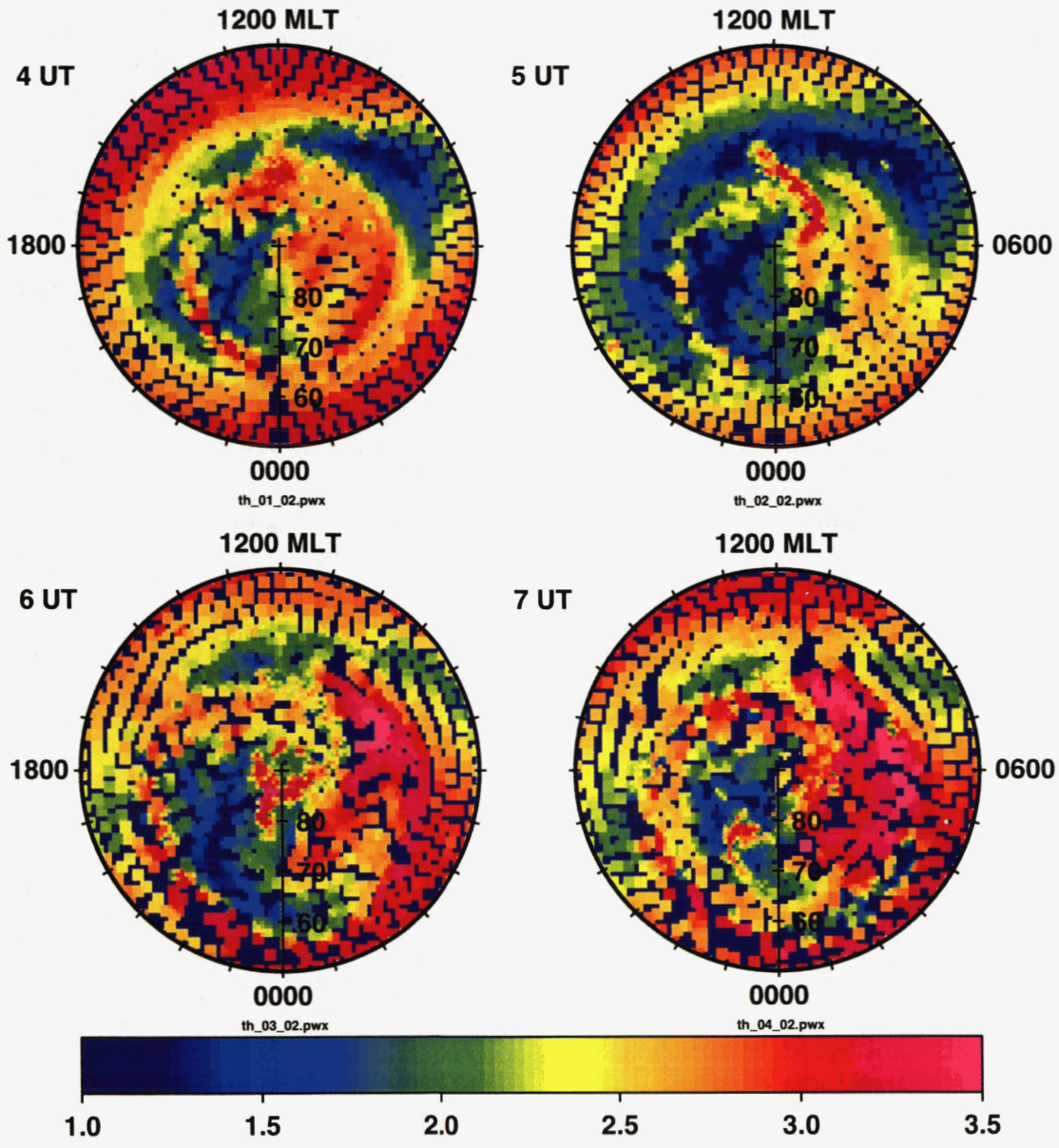

Figure 6. Snapshots of the H^+ density distribution at 1000 km and at selected times (4, 5, 6, and 7 UT) during the ionosphere-polar wind simulation. The dial plots cover magnetic latitudes greater than 50° and the color bar gives values of $\log_{10} n(H^+)$, with $n(H^+)$ in cm^{-3}. The granularity of the plots is due to the spatial resolution associated with the number of convecting flux tubes (1500) used in the simulation. From Paper 21.

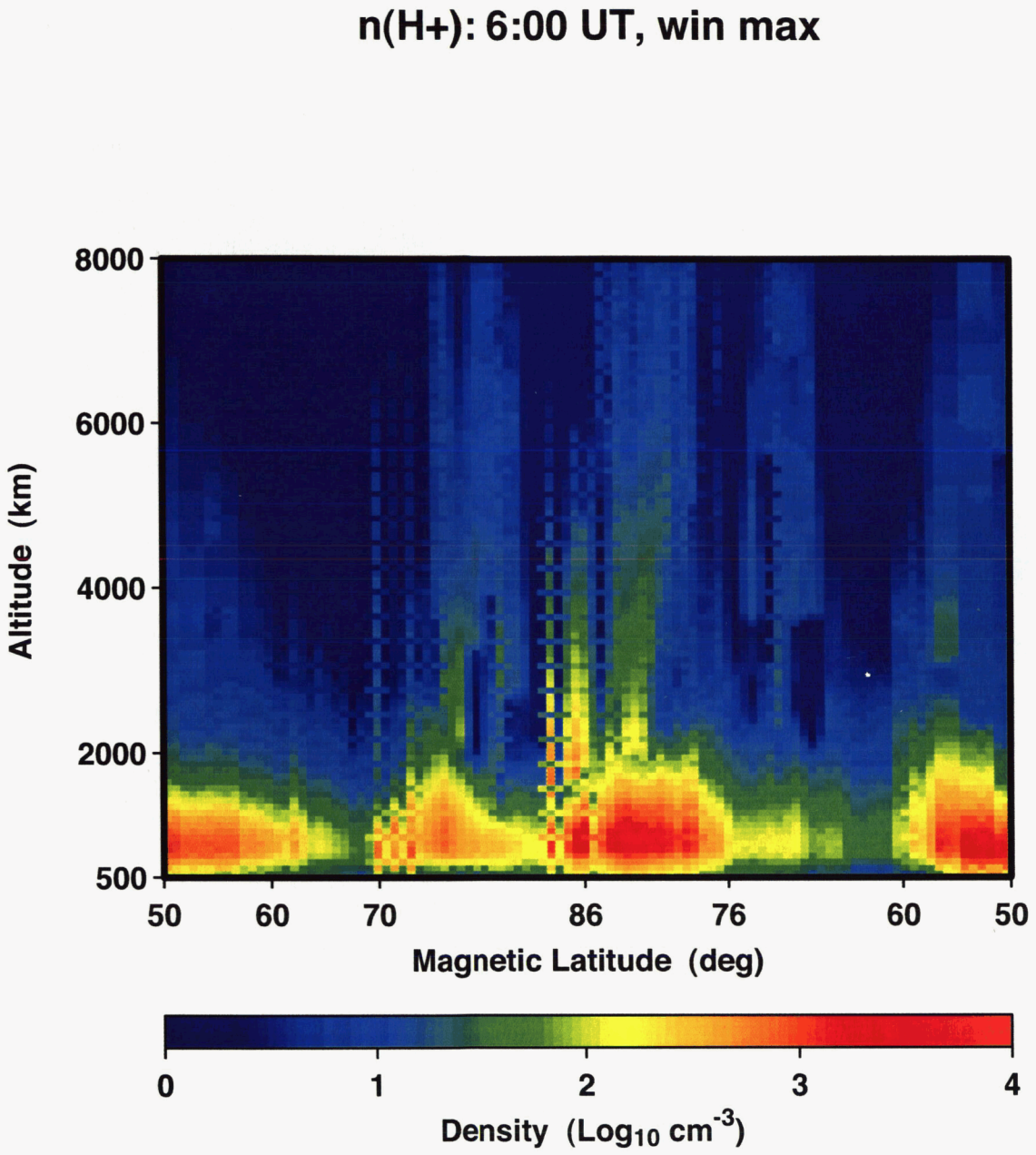

Figure 7. Snapshots of the H^+ density distribution versus altitude and magnetic latitude at 6 UT. From Paper 21.

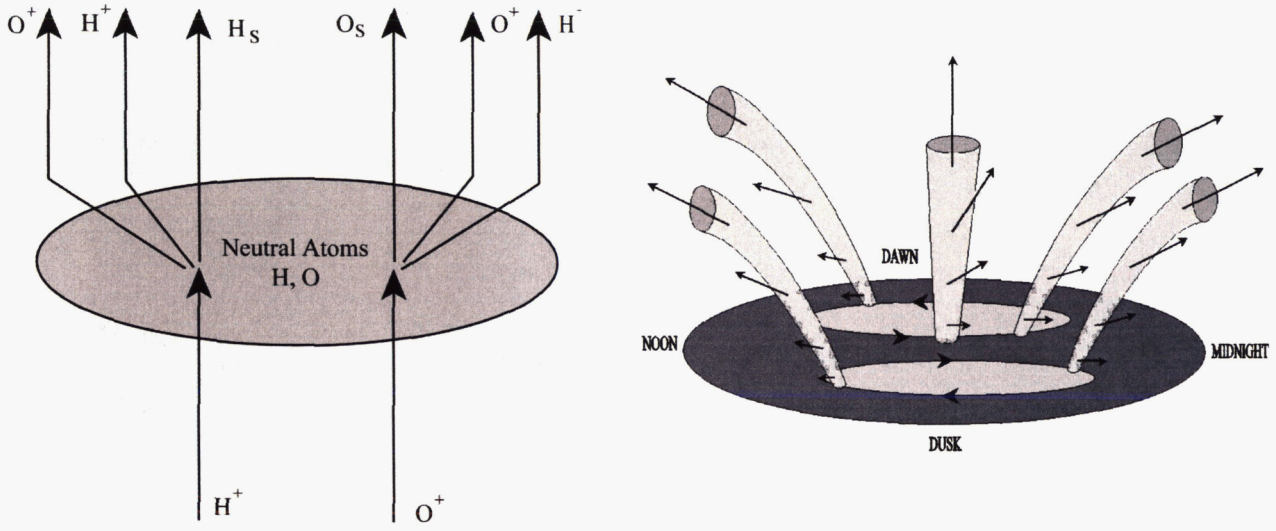

Figure 8. Schematic diagram showing the production mechanism for the neutral stream particles as the upflowing polar wind traverses a background neutral atmosphere (left panel). The right panel is a schematic diagram that shows the 3-dimensional nature of the neutral polar wind and the production of low-energy neutrals flowing in all directions. From Paper 22.

systematic modeling studies in order to determine their quantitative effect. Our studies are based on a *time-dependent, high-resolution* model of the *global* thermosphere that we developed several years ago. In one study, we focused on the effects that theta aurora have on the thermosphere (Paper 20).

Polar cap arcs are discrete 630-nm emission structures in the polar cap. The arcs appear when the IMF is near zero or northward and are a result of electron precipitation, with the characteristic energy varying from 300 eV to 5 keV and the energy flux varying from 0.1 to a few erg cm^{-2} s^{-1}. They are relatively narrow, but are extended along the noon-midnight direction (1000-3000 km). For a strongly northward IMF, a single arc can form that extends all the way from the dayside to the nightside auroral oval, with the associated optical emission appearing as the Greek letter theta when viewed from space.

In order to determine the effect of transpolar arcs on the polar thermosphere, simulations were conducted both with and without transpolar arcs using the USU Thermosphere General Circulation Model (TGCM). Simulations were conducted for different background geophysical conditions and different transpolar arc characteristics. Figure 9 shows the neutral mass density and temperature perturbations due to a transpolar arc that is associated with a theta aurora. For this case, the arc was assumed to be stationary and to be 500 km wide. The ionospheric density enhancement in the arc was assumed to vary across the arc, from a peak value at the arc's center to the background ionospheric density at the edges of the arc. For Figure 9, the peak electron

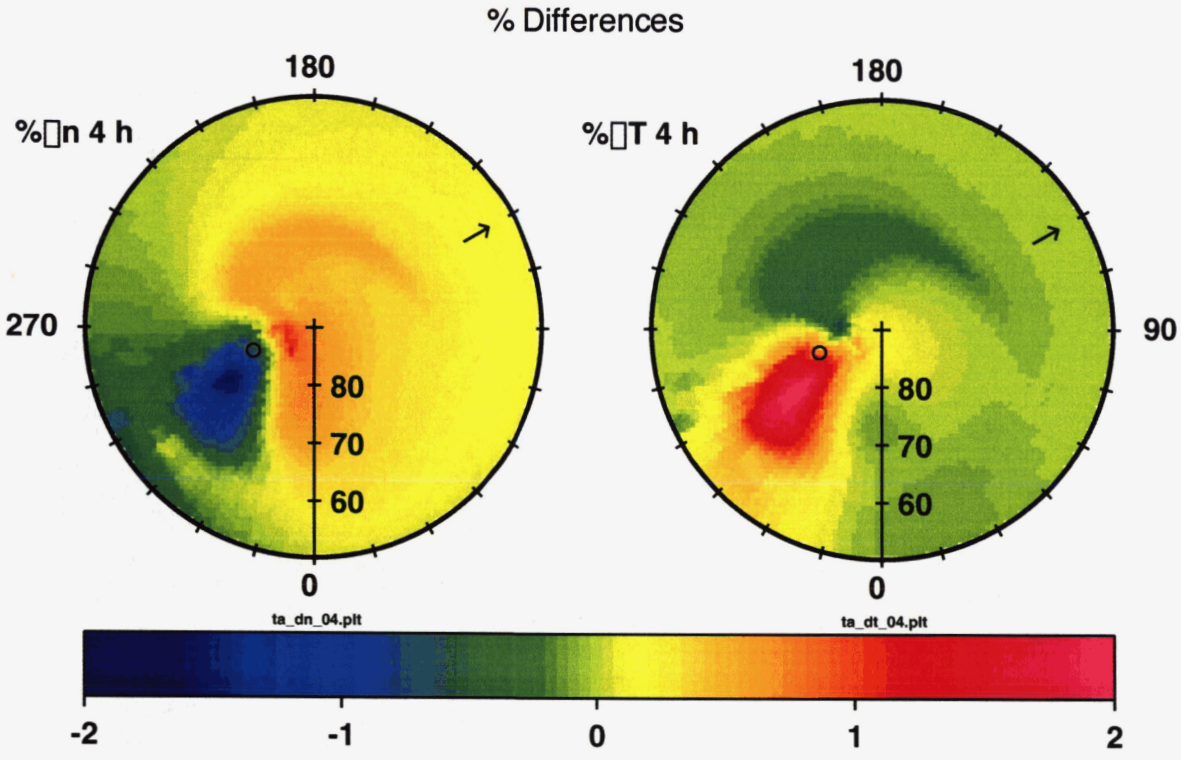

Figure 9. Thermospheric mass density (left panel) and temperature (right panel) perturbations due to the presence of a transpolar arc that is associated with a theta aurora. From Paper 20.

density at the arc's center was a factor of 10 above the background electron density. The geophysical conditions correspond to moderate solar activity ($F_{10.7}$ = 150), winter, and northward IFM (8 nT). The left panel shows the percentage change of the perturbed neutral mass density and the right panel shows the corresponding neutral temperature perturbation. These perturbations were calculated by subtracting the values for the simulation without the transpolar arc from the values for the simulation that included the transpolar arc. For a theta aurora that persists for four hours, the overall neutral mass density and temperature perturbations from the enhancements to the depletions vary from 3-4%.

Ionosphere-Magnetosphere Coupling → Small-Scale Auroral Structuring

The auroral structures on the spatial scales of 10s-100s km and their associated electrodynamics are key elements in the magnetosphere-ionosphere (M-I) system and are important for ionospheric dynamics. The simulation of these auroras poses a challenge for global magnetohydrodynamic (MHD) M-I models. In a recent study (Paper 17), we proposed an M-I coupling mechanism for the formation of auroral structures on these spatial scales. In the M-I coupling mechanism, the active role of the ionosphere was taken into account and the auroral structures with spatial scales of 10s-100s km, which do not mirror the scales of the

magnetospheric drivers, self-consistently developed. The proposed mechanism includes the effects of the ionospheric spatial and temporal scales and the M-I coupling processes. By calculating the reflection of the Alfvén waves at the ionosphere and the Alfvén waves launched by the temporal variation of the ionospheric conductivity, the mechanism provided time-dependent, quantitative information of all electrodynamic parameters associated with the dynamic evolution of structured auroras, including the field-aligned currents, ionospheric horizontal currents, convection field, conductivity, and Joule heating rate. The M-I coupling mechanism has been quantitatively tested and validated by using numerical simulations and model-observation comparisons. Some of the theoretical predictions have been independently confirmed by observations. With its strengths of (a) quantitative capability and (b) emphasis on the active role of the ionosphere, this M-I coupling mechanism complements other mechanisms for the auroral structures as well as the global MHD M-I modeling, thus improving our understanding of the auroral structures and the M-I coupling processes.

Ionosphere-Magnetosphere Coupling → Auroral Ion Energization

The effects of low-altitude energization (LAE) of ions in the auroral region are being investigated using a 3-D dynamic model (Paper 24). In this study, we simulate the behavior of a large number (~100 to 1000) of plasma-filled geomagnetic tubes. The model is composed of two components. The high-altitude component is based on a macroscopic particle-in-cell (mac-PIC) approach that extends from an altitude of 1200 km to several Earth radii. The lower boundary conditions of the mac-PIC model are provided by a 3-D fluid-like model (low-altitude component) that extends down to 100 km in altitude. The total number of simulation particles in the mac-PIC component is more than 10^8. The generalized polar wind is followed for about 12 hours with a time step of 2.5 seconds. The computing-intensive nature of the model requires utilization of supercomputers with ~100 to 1000 processors. A 3-D picture is assembled from the temporal evolution of the individual flux tubes by keeping track of their locations. The resulting 3-D dynamic picture is investigated with special emphasis on the role that the LAE plays. The main conclusions are: (1) In the absence of LAE, the dominant source of escaping O^+ occurs within the polar cap due to the influence of magnetospheric electrons; (2) Both upward and downward O^+ fluxes occur at low altitudes, while only upward O^+ fluxes occur at high altitudes; and (3) Downward O^+ fluxes occur essentially during the storm recovery phase, at the equatorward edge of the polar cap within the dawn-noon sector.

Recent SEC Theory Publications

The following is a list of publications that were supported, in part, by NASA Grant NAG5-11880.

1. Barakat, A. R., and R. W. Schunk, Effects of wave-particle interactions on the dynamic behavior of the generalized polar wind, *J. Atmos. Solar-Terr. Phys., 63,* 75-83, 2001.
2. Ma, T.-Z., and R. W. Schunk, The effects of multiple propagating plasma patches on the polar thermosphere, *J. Atmos. Solar-Terr. Phys., 63*, 355-366, 2001.
3. Schunk, R. W., Ionospheric climatology and weather disturbances, *AGU Monograph on Space Weather, 125*, 359-368, 2001.
4. Sojka, J. J., R. W. Schunk, M. David, J. L. Innis, P. A. Greet, and P. L. Dyson, A theoretical model study of F-region response to high latitude neutral wind upwelling events, *J. Atmos. Solar-Terr. Phys., 63*, 1571-1584, 2001.
5. Demars, H. G., and R. W. Schunk, Seasonal and solar-cycle variations of the polar wind, *J. Geophys. Res., 106*, 8157-8168, 2001.
6. Schunk, R. W., Ionospheric models: Earth, in *Comparative Aeronomy in the Solar System, Geophysical Monograph, 130*, 299-306, 2002.
7. Schunk, R. W., L. Scherliess, and J. J. Sojka, Ionospheric specification and forecast modeling, *J. Spacecraft and Rockets, 39*, 314-324, 2002.
8. Sojka, J. J., M. David, and R. W. Schunk, A mid-latitude space weather hazard driven directly by the magnetosphere, *J. Atmos. Solar-Terr. Phys., 64*, 687-695, 2002.
9. David, M., J. J. Sojka, R. W. Schunk, and R. A. Heelis, Relative solar and auroral contribution to the polar F-region: Implications for National Space Weather Program, *J. Geophys. Res., 107*, A10, 1310, doi:10.1029/2001JA009167, 2002.
10. Demars, H. G., and R. W. Schunk, Three-dimensional velocity structure of the polar wind, *J. Geophys. Res., 107*, 1250, doi:10.1029/2001JA000252, 2002.
11. Schunk, R. W., L. Scherliess, and J. J. Sojka, Recent approaches to modeling ionospheric weather, *Adv. Space Res., 31*, 819-828, 2003.
12. Barakat, A. R., R. W. Schunk, and H. G. Demars, Seasonal and solar cycle dependence of the generalized polar wind with low-altitude auroral ion energization, *J. Geophys. Res., 108* (A11), 1405, doi:10.1029/2002JA009360, 2003.
13. Cade, III, W. B., J. J. Sojka, L. Zhu, and Y. Kamide, A wavelet analysis of storm/substorm relationship, *Disturbances in Geospace: The Storm/Substorm Relationship, Geophysical Monograph 142,* 159, 2003.
14. Zhu, L., Substorms, in *Encyclopedia of the Arctic* (ed. M. Nuttall), Fitzroy Dearborn Publishers, England, 2003.

15. Zhu, L., R. W. Schunk, and J. J. Sojka, Alfvén waves of ionospheric origin and the associated plasma dynamics and electrodynamics, *Proceedings of the XXVII URSI Assembly*, 2002.

16. Schunk, R. W., and H. G. Demars, Effect of equatorial plasma bubbles on the thermosphere, *J. Geophys. Res., 108* (A6), 1245, doi:10.1029/2002JA009690, 2003.

17. Zhu, L., J. J. Sojka, and R. W. Schunk, Active ionospheric role in small-scale auroral structuring, *J. Atmos. Solar-Terr. Phys., 67*, 687-700, 2005.

18. Zhu, L., R. W. Schunk, and J. J. Sojka, Modeling ground magnetic disturbance during substorms, *J. Geophys. Res.*, draft manuscript, 2004.

19. Zhu, L., R. W. Schunk, and J. J. Sojka, Model study of the ionosphere-originated field-aligned currents and electric field structures, *J. Geophys. Res.*, draft manuscript, 2004.

20. Demars, H. G., and R. W. Schunk, Effect of the theta aurora on the polar thermosphere, *J. Atmos. Solar-Terr. Phys., 67*, 489-499, 2005.

21. Schunk, R. W., H. G. Demars, and J. J. Sojka, Propagating polar wind jets, *J. Atmos. Solar-Terr. Phys., 67*, 357-364, 2005.

22. Gardner, L. C., and R. W. Schunk, Neutral polar wind, *J. Geophys. Res., 109*, A05301, doi:10.1029/2003JA010291, 2004.

23. Barghouthi, I. A., and A. R. Barakat, A Monte Carlo study of a generalized Coulomb Milne problem, draft manuscript, 2004.

24. Barakat, A. R., and R. W. Schunk, 3-D dynamic behavior of the generalized polar wind with low-altitude auroral ion energization, in preparation, 2004.

25. Sojka, J. J., M. David, R. W. Schunk, and T. van Eyken, Polar F-layer model-observation comparison: A neutral wind surprise, *Annales Geophysicae, 23,* 191-199, 2005.

26. Schunk, R. W., Time-dependent simulations of the global polar wind, *J. Atmos. Solar-Terr. Phys.*, in press, 2005.

27. Gardner, L., and R. W. Schunk, Global neutral polar wind model, *J. Geophys. Res.*, in press, 2005.

28. Gardner, L., and R. W. Schunk, 3-D neutral polar wind, *Adv. Space Res.*, in press, 2005.